Published in final edited form as:
Clin Cancer Res. 2011 December 15; 17(24): 7634–7644. doi:10.1158/1078-0432.CCR-11-1677.

Pharmacodynamic Study Using FLT PET/CT in Patients with Renal Cell Cancer and Other Solid Malignancies Treated with Sunitinib Malate

Glenn Liu[1,2,3,*], **Robert Jeraj**[1,2,4,5,*], **Matt Vanderhoek**[4], **Scott Perlman**[1,2,5], **Jill Kolesar**[1,6], **Michael Harrison**[1,2,3], **Urban Simoncic**[4], **Jens Eickhoff**[1,7], **Lakeesha Carmichael**[1,7], **Bo Chao**[3], **Rebecca Marnocha**[1,6], **Percy Ivy**[8], and **George Wilding**[1,3]

[1]University of Wisconsin Carbone Cancer Center

[2]Translational Imaging Research Group

[3]Department of Medicine, Division of Hematology/Oncology

[4]Department of Medical Physics

[5]Department of Radiology

[6]School of Pharmacy

[7]Department of Biostatistics

[8]Cancer Therapy Evaluation Program, National Cancer Institute

Abstract

Purpose—To characterize proliferative changes in tumors during the sunitinib malate exposure/withdrawal using 3′-Deoxy-3′-[^{18}F]fluorothymidine (FLT) PET/CT imaging.

Patients and Methods—Patients with advanced solid malignancies and no prior anti-VEGF exposure were enrolled. All patients had metastatic lesions amenable to FLT PET/CT imaging. Sunitinib was initiated at the standard dose of 50 mg PO daily either on a 4/2 or 2/1 schedule. FLT PET/CT scans were obtained at baseline, during sunitinib exposure, and after sunitinib withdrawal within cycle #1 of therapy. VEGF levels and sunitinib pharmacokinetic data were assessed at the same time points.

Results—16 patients (8 pts on 4/2 schedule; 8 pts on 2/1 schedule) completed all three planned FLT PET/CT scans, and were evaluable for pharmacodynamic imaging evaluation. During sunitinib withdrawal (change from scan 2 to 3), median FLT PET SUV_{mean} increased +15% (range −14% to +277%) (p=0.047) for the 4/2 schedule and +19% (range −5.3% to +200%) (p=0.047) for the 2/1 schedule. Sunitinib PK and VEGF ligand levels increased during sunitinib exposure, and returned towards baseline during the treatment withdrawal.

Conclusions—The increase of cellular proliferation during sunitinib withdrawal in patients with renal cell carcinoma and other solid malignancies is consistent with a VEGFR TKI withdrawal flare. Univariate and multivariate analysis suggest that plasma VEGF is associated with this flare, with an exploratory analysis implying that patients who experience less clinical benefit have a

Address all correspondence to: Glenn Liu, MD, University of Wisconsin Carbone Cancer Center, Wisconsin Institutes for Medical Research, Room 7051, 1111 Highland Avenue, Madison, Wisconsin 53705, Fax 608-265-0614; Phone 608-265-8689, gxl@medicine.wisc.edu.
*Contributed equally to this work

ClinicalTrials.gov Identifier: NCT00499125

larger withdrawal flare. This might suggest that patients with a robust compensatory response to VEGFR TKI therapy experience early “angiogenic escape”.

Keywords

Angiogenesis; molecular imaging; VEGFR TKI

Introduction

In 1971, Judah Folkman hypothesized that angiogenesis plays an integral role in tumor growth.(1) As a result, inhibiting angiogenesis was considered a reasonable strategy to prevent tumor progression and metastasis. Currently, the vascular endothelial growth factor (VEGF) signaling pathway is the best-described target for anti-angiogenic treatment. Since 2004, multiple VEGF signaling pathway (VSP) inhibitors have been approved by the US Food and Drug Administration (FDA) based on improvements in overall survival (OS) and/or progression-free survival (PFS) validating this target. The first of these drugs approved was bevacizumab, a humanized monoclonal antibody against VEGF. While its single-agent activity in most solid malignancies was low,(2, 3) it is approved for use in metastatic colorectal cancer (CRC)(4, 5) and non-small cell lung carcinoma (NSCLC)(6) due to improvements in OS when combined with cytotoxic chemotherapy. In comparison, newer agents that target the VEGF receptor (VEGFR) tyrosine kinase inhibitor (TKI) have resulted in higher single-agent activity compared to bevacizumab. Multiple VEGFR TKIs, including sorafenib, sunitinib, and pazopanib, are now approved as monotherapy in metastatic renal cell carcinoma (mRCC),(7–11) and gastrointestinal stromal tumors.(12) Despite relatively modest OS improvements, all of these clinical studies confirm that targeting angiogenesis is a validated treatment strategy.

Sunitinib malate is a receptor tyrosine kinase inhibitor (TKI) that exerts its key mechanism of action in mRCC through inhibition of VEGF receptors (VEGFR) -1, -2, and -3 and platelet derived growth factor receptors (PDGFR) -α and -β on tumor vascular endothelium.(13) The approved schedule is 50 mg by mouth daily for 4 weeks followed by a 2 week break (4/2 schedule); however, sunitinib has also been studied on a 2/1 schedule.(14) In treatment-naïve mRCC patients, a randomized phase III trial demonstrated improved median progression-free survival with sunitinib with an investigator-reported objective response rate (ORR) for sunitinib of 47% (3% complete responses).(10) Reports in the literature of CRs in mRCC patients treated with sunitinib have remained consistently low.(15–17) In contrast to sunitinib, single-agent bevacizumab appears to produce a relatively modest ORR and PFS of 10 to 13% and 4.8 to 8.5 months, respectively.(18, 19) Overall, all patients eventually progress on anti-angiogenic therapy. This has generated many questions as to how patients become resistant to anti-angiogenic drugs and led many investigators to empirically combine sunitinib with other agents in an attempt to prolong benefit.

We have observed that patients with mRCC treated with sunitinib on the 4/2 schedule can achieve clinical improvement in sites of painful metastases during sunitinib exposure, but can develop recurrent pain within 4 to 5 days of stopping sunitinib. We suspected that this VEGFR TKI withdrawal flare may be associated with a period of rapid, transient tumor re-growth,(20, 21) and that the pain would decrease with resumption of therapy. We suggested that during this “flare,” the tumor would be more engaged in S-phase of the cell cycle (proliferation) and thus more responsive to cytotoxic chemotherapy. However, several key questions remain: 1) whether the VEGFR TKI withdrawal flare is common; 2) whether it is specific to clear cell renal cell carcinoma, as opposed to other solid tumor types; and 3) whether the flare represents a true increase in tumor cell proliferation (instead of an inflammatory or vascular effect). Based on our clinical observations and available clinical

trial and preclinical data, we hypothesized that there is a period of rapid tumor progression in most solid tumors following acute cessation of sunitinib. This study was designed to explore this hypothesis by using molecular imaging to better understand the pharmacodynamic changes with sunitinib. As sunitinib is administered using an "intermittent" schedule, it allows imaging assessment both during treatment exposure and during acute treatment withdrawal. Better understanding of the pharmacodynamic changes with sunitinib would also provide necessary understanding to test the second hypothesis of synergistic combination of VEGFR TKI with cytotoxic therapy.

3′-Deoxy-3′-[^{18}F]fluorothymidine (FLT) is a tracer used for imaging tumor proliferation by positron emission tomography (PET).(22–26) Direct correlation between FLT uptake and proliferation as assessed by Ki-67 labeling index has also been observed when full kinetic analysis is performed.(27–30) As a result, use of FLT PET/CT scanning was ideal for this study, as it allowed non-invastive assessment of proliferation pharmacodynamics (PD) in patients treated with sunitinib.

This study was designed and conducted at the University of Wisconsin Carbone Cancer Center. The goal was to use FLT PET/CT to characterize and quantify changes in tumor proliferation during sunitinib exposure and temporary withdrawal, explore pharmacodynamic changes that may yield insight into predicting treatment response/failure, and gain further insight regarding the physiologic effects of VEGFR TKI in patients with advanced malignancies. In addition to clinical outcomes, the aim was to correlate FLT PET/CT imaging results with both sunitinib pharmacokinetic (PK) and plasma VEGF levels as potential explanations for the withdrawal flare.

Patients and Methods

Patient Selection

Patients were required to have histologically or cytologically confirmed renal cell cancer or any other solid malignancy (excluding lymphoma) that was metastatic or unresectable and for which no standard curative therapy existed. For the renal cell cancer subset, a component of clear cell histology was required. Other key inclusion criteria included: measurable disease by RECIST 1.0 guidelines,(31) appropriate target lesions for FLT PET/CT assessment (minimum 1.5 cm, located in a region of body with low motion artifact, reasonable ability to delineate tumor boundaries on CT and PET, non-hepatic due to high background FLT uptake), controlled blood pressure (<140/90 mmHg) at enrollment, and normal organ and bone marrow function. Patients with prior anti-VEGF treatment (for example, bevacizumab or VEGFR TKI) were excluded, as were patients taking inducers or moderate or strong inhibitors of the CYP3A4 liver enzyme. All patients signed informed consent documents approved by the Institutional Review Board at the University of Wisconsin. Additional approval by the Radioactive Drug Research Committee at the University of Wisconsin was obtained given use of an experimental tracer. This study was conducted in accordance with the Declaration of Helsinki.

Drug Administration and Study Design

Sunitinib was supplied in 12.5 mg, 25 mg, and 50 mg capsules. Two treatment schedules were assessed (Figure 1). On Treatment Schedule A (*4/2 schedule*), patients initially took one 50 mg capsule of sunitinib daily for 4 consecutive weeks followed by 2 weeks (drug withdrawal) with no sunitinib (6 week cycle). On Treatment Schedule B (*2/1 schedule*), patients took one 50 mg capsule of sunitinib daily for 2 consecutive weeks followed by 1 week (drug withdrawal) with no sunitinib. This 2/1 schedule was administered every 3 weeks (repeated once) during the 6 week cycle. Pharmacodynamic and pharmacokinetic

time points, described in greater detail below and depicted in Figure 1, included: (1) *baseline* (before sunitinib treatment), (2) *maximum sunitinib exposure* (near end of consecutive dosing period), and (3) *maximum sunitinib washout* (near end of drug withdrawal period).

FLT PET/CT Imaging

In order to minimize uncertainties inherent in PET imaging, strict imaging procedures were followed, including: employing optimized and standardized image acquisition and reconstruction protocols, and performing comprehensive image analysis procedures. At the beginning of each imaging session, a CT scan was obtained on a Discovery LS (General Electric, Waukesha, WI) PET/CT scanner. Dynamic PET imaging was performed for the first 30 minutes over the pre-defined region (15 cm field of view) to obtain necessary data for kinetic analysis. After the dynamic scan, a static whole body scan (6 scanning positions ~ 90 cm total length) was initiated at 60 minutes post injection. All scans were acquired in a 2D mode, and reconstructed on a 256×256 reconstruction grid using OSEM iterative reconstruction algorithm with 5 mm post-filtering. The dynamic FLT PET/CT imaging data was used to perform kinetic analysis of the imaging data, thus allowing increased correlation to the biological parameters (cell proliferation index) and extraction of vasculature data (e.g., perfusion/permeability, blood volume). The static whole body FLT PET/CT imaging data was employed to identify primary tumor and metastases. The CT data was analyzed to establish anatomical changes in tumor size. Each metastasis was identified by an experienced nuclear medicine physician and segmented using a combination of semi-automatic segmentation methods using Amira (Visage Imaging Inc, San Diego, CA) software, with up to five metastases used in image analysis. As the whole body kinetic analysis is impractical, we performed analysis on various standardized uptake value (SUV) measures of FLT uptake. SUV_{mean}, SUV_{max}, SUV_{peak} and SUV_{total} were recorded and analyzed. Multiple SUV measures were investigated to capture intra-lesion response heterogeneity (e.g., most proliferative parts of the tumor (SUV_{max}) might not respond, even though tumor as whole (SUV_{mean}) does respond). In order to cross-validate our results, FLT PET SUV measures were compared to measures extracted from the full kinetic analysis. All image analysis was performed at the University of Wisconsin Image Analysis Core (IMAC) facility.

Sunitinib Pharmacokinetic and Plasma VEGF

Plasma pharmacokinetic (PK) levels of sunitinib were drawn prior to initiating sunitinib therapy on day 1 and on the days PET scans were performed. In order to monitor changes in serum VEGF levels, samples were collected: on day 1 prior to dosing, weekly during cycle 1, and on day 1 of each subsequent cycle.

Plasma VEGF levels were evaluated using a commercially available 96-well plate quantitative sandwich immunoassay (Quantikine human VEGF, R & D Systems, Minneapolis, MN). Sunitinib and the active metabolite SU12662 in plasma were evaluated by LCMSMS as previously described.(32) The analytical system consisted of an HPLC coupled directly to a model API 4000 triple quadrupole mass spectrometer equipped with a Turbo V™ atmospheric pressure ionization source fitted with the electrospray probe (Applied Biosystems/MDS Sciex, Concord, Ontario, Canada). The assay was validated in our laboratory and demonstrated a linear range of 3.12 – 100 ng/ml with $r^2 = 0.998$, with an intraday variability of 3.37% for sunitinib and 6.55% for SU12662. Interday variability was 2.20%/4.03% for the low sunitinib/SU12662 standard of 6.25/3.12 ng/ml; it was 0.45%/ 0.99% for the 100/50 ng/mL. The LLOQ was 3.12 ng/ml for both sunitinib and SU12662. Recovery based on standard addition was 98.3% for sunitinib and 93.6% for SU12662.

Treatment Response Evaluation

Patients were evaluated for response and progression after every two cycles (every 12 weeks) of therapy using RECIST 1.0 guidelines.(31) Those with complete response (CR) or partial response (PR) as the best response by RECIST were classified as *objective responders*. Those with stable disease (SD) or progression of disease (PD) as the best response by RECIST were classified as *objective non-responders*.

An exploratory, unplanned analysis was added to categorize patients by clinical benefit status (yes/no). Patients who discontinued sunitinib prior to month 6 for any reason (including progression, toxicity, patient/physician discretion, etc.) were categorized as having *no clinical benefit* (NCB) and those who remained on sunitinib at or after 6 months were categorized as having *clinical benefit* (CB). Given the heterogeneous patient population (different tumor types, variable prior therapies received, etc.) in this pharmacodynamic trial, this endpoint of clinical benefit was felt to capture additional information not included in the objective response status. The objective response and clinical benefit status were correlated with pharmacodynamic FLT PET imaging data.

Statistical Methods

The study was powered to detect a mean change of 33% in the SUVs parameters at the 5% significance level, assuming an anticipated standard deviation ranging from 20 to 30%. A sample size of 10 evaluable patients was planned for each of the two treatment schedules. With a sample size of 10 evaluable patients per treatment schedule, an anticipated mean change of 33% in the SUVs parameters would have been detected with 87% power at the two-sided 5% significance level, assuming a standard deviation of 30%. We anticipated a drop-out rate of up to 20% and, hence, accrued a total of 25 patients.

FLT PET imaging PD measures, plasma VEGF and PK levels of sunitinib and its metabolite were summarized in terms of medians and ranges for each assessment time point. As the distribution of FLT PET SUV values are known to be left-skewed,(33) non-parametric tests were utilized for performing statistical inference and median profile plots were used to represent the data graphically. Specifically, changes from baseline were evaluated using a nonparametric Wilcoxon signed rank test. Associations between changes in the various PK and imaging PD parameters were analyzed using Spearman's rank correlation (r_s) analysis. Furthermore, in order to adjust the associations between changes in PD parameters for changes in sunitinib concentration, partial Spearman's rank correlation analysis (r_{ps}) was conducted. The comparison of changes in PD parameters between responders and non-responders was performed using a nonparametric Wilcoxon rank test. All analyses were performed using SAS software version 9.2 (SAS Institute, Cary, NC). All statistical tests were two-sided and P-values less than 0.05 were considered statistically significant.

Results

Patient Characteristics

From June 2007 to September 2009, 25 patients were enrolled at the University of Wisconsin Carbone Cancer Center. To be evaluable for PK/PD analysis, a patient must have taken the full cycle of sunitinib as planned and received a set of all 3 FLT PET/CT scans of adequate quality. Of 25 enrolled patients, 16 were evaluable. Technical problems, which included radiotracer instability and the cyclotron going offline, resulted in 2 patients not receiving the first FLT PET/CT scans. An additional 7 patients who received at least one FLT PET/CT scan were unevaluable for various reasons (FLT production not meeting quality control standard, PET/CT problem, treatment tolerability, etc.), leaving eight

evaluable patients each in both treatment schedules. One patient with mRCC (systemic treatment-naïve) on the 2/1 schedule remains on study after 22 cycles of therapy.

Median age was 60 (range: 42 – 76), while 75% of subjects were male. As specified by the protocol, nearly half (n = 7) of evaluable patients had mRCC (4/2 schedule: n = 5; 2/1 schedule: n = 2). The remainder represented a diverse group of tumor types: esophagus (n = 2), liver (hepatocellular; n = 2), prostate (n = 1), sarcoma (n = 1), small cell lung (n = 1), thymus (n = 1), and uterine carcino-sarcoma (n = 1). Six of seven patients with mRCC had prior nephrectomy. The median number of prior systemic therapy regimens was 1 (range: 0 – 4). All subjects were naïve to anti-VEGF therapy, as specified by the protocol. Seven subjects (44%) had been treated with prior chemotherapy, while 3 subjects (19%) had received investigational treatment. One subject with mRCC had undergone treatment with an investigational agent and immunotherapy with interleukin-2, whereas the other 6 patients with mRCC were systemic treatment-naïve.

FLT PET/CT Imaging (Table 1, Figures 2 and 3)

Figure 2 shows examples of the tumor flare phenomenon on FLT PET/CT in various tumor types. Quantitative assessment of the FLT PET/CT imaging parameters are summarized in Table 1 and Figure 3. Even though the comprehensive image analysis included many imaging parameters, we report here only the *mean* standardized uptake value (SUV_{mean}) and *maximum* standardized uptake value (SUV_{max}) because these likely represent distinct parameters of cellular proliferation distribution. The average pre-treatment SUV_{mean} across patient population was 3.2 (range 1.4–7.9), decreasing to 2.1 (range 0.6–3.8) and rebounding back to 3.1(range 0.7–8.3). The average pre-treatment SUV_{max} across patient population was 10.1 (range 4.1–30.2), decreasing to 6.0 (range 1.5–13.4) and rebounding back to 10.1 (range 2.6–32.1). Note that all the SUV data used was normalized to the pretreatment scan for each patient, as the overall objective was to quantify the treatment response dynamics through sunitinib treatment and withdrawal.

For SUV_{mean}, there was a statistically significant decrease during sunitinib treatment on the 4/2 schedule (−16%; p = 0.031), but not on the 2/1 schedule (−18%; p = 0.109). There were statistically significant increases in SUV_{mean} during sunitinib withdrawal (4/2 schedule: +15%; p = 0.047; 2/1 schedule: +19%; p = 0.047). Note that the range of individual responses was significant and exceeded 100%. For SUV_{max}, there were statistically significant decreases during sunitinib treatment (4/2 schedule: −34%; p = 0.016, 2/1 schedule: −21%; p = 0.039). However, there was only a trend toward a statistically significant increase in SUV_{max} during sunitinib withdrawal (4/2 schedule: + 33%; p = 0.078; 2/1 schedule: +28%; p = 0.109). Similarly for SUV_{max} the range of responses was significant and exceeded 100%. When treatment groups were combined, there was a statistically significant decrease in both SUV_{mean} and SUV_{max} during sunitinib treatment (p = 0.001 and p = 0.002, respectively). Likewise, there was a statistically significant increase in SUV_{mean} and SUV_{max} during sunitinib withdrawal when both treatment groups were combined (p = 0.011 and p = 0.004, respectively). The trends of the FLT PET kinetic macroparameter K_i, representing the proliferation rate, were in concordance with the trends of the FLT PET SUV measures.

Sunitinib Pharmacokinetics and Plasma VEGF (Table 1 and Figure 3)

The median change from baseline in plasma sunitinib concentrations between baseline and the second PET/CT scan was 63 ng/mL (range 37–184 ng/mL) in the 4/2 cohort and 62 ng/mL (range 32–162 ng/mL) in the 2/1 cohort. The median change from the baseline in plasma sunitinib metabolite concentrations were 20 ng/mL (range 14–39 ng/mL) in the 4/2 cohort and 21 ng/mL (range 4.8–52 ng/mL) in the 2/1 cohort. After sunitinib withdrawal, and at the

time of the third PET/CT scan, plasma concentrations declined to near baseline levels. Changes in levels of sunitinib and its metabolite were statistically significant during both the exposure and withdrawal period and in both treatment groups.

Plasma VEGF increased during sunitinib exposure in both treatment groups, as expected. Likewise, plasma VEGF decreased during sunitinib withdrawal in both treatment groups. Changes in plasma VEGF were statistically significant during the exposure and withdrawal period and in both treatment groups.

Objective Response Evaluation

There were 16 total patients evaluable for objective response per RECIST 1.0, with an overall objective response rate of 36% (95% CI: 16–61%). The response rate (partial response) for the 4/2 schedule (n = 8) was 38% and the response rate for the 2/1 schedule (n = 8) was 33%. No complete responses were observed. Of the 16 patients evaluable for FLT PET/CT imaging, only 14 of the patients were evaluable for objective response per RECIST 1.0. Of the two unevaluable patients, one patient with esophageal cancer was taken off study before the planned week 12 disease assessment secondary to a cerebral vascular accident. The second patient (uterine carcino-sarcoma) withdrew consent after 48 days of study participation for personal reasons.

Correlation Between PK, PD, and Response Parameters

The Spearman's rank correlations (r_s) for the changes from baseline to the end of the treatment and withdrawal period between the various PK and PD parameters (i.e. sunitinib concentration, VEGF, SUV) were calculated and are shown in Table 2. Statistically significant negative correlations were observed between VEGF and SUV_{mean}, and VEGF and SUV_{max} during sunitinib treatment on the 4/2 treatment schedule: $r_s = -0.92$ ($p = 0.003$) and $r_s = -0.79$ ($p = 0.036$), respectively.

Parameters were also analyzed with the two groups combined. After adjusting for sunitinib concentration in the combined group, VEGF was found to be negatively correlated with both SUV_{mean} and SUV_{max} during sunitinib treatment with partial Spearman's rank correlations of $r_{ps} = -0.69$ ($p = 0.0041$) and $r_{ps} = -0.71$ ($p = 0.0030$), respectively. Similarly, VEGF was found to be negatively correlated with both SUV_{mean} and SUV_{max} during sunitinib withdrawal after adjusting for sunitinib concentration in the combined group ($r_{ps} = -0.82$, $p = 0.0002$; $r_{ps} = -0.85$, $p = 0.0001$). Multivariate analysis, involving both changes in VEGF and sunitinib concentration as predictors for changes in SUV_{mean}, showed that changes in VEGF independently predicted change in SUV_{mean} during the sunitinib treatment period ($p = 0.003$).

Furthermore, the association between changes in pharmacodynamic parameters and clinical response was evaluated. When both treatment groups were combined, *objective non-responders* (n = 9) had statistically significant median increases in SUV_{mean} (+29%, range: −5 to +277%; $p = 0.012$) and SUV_{max} (+36%, range: −11 to +221%; $p = 0.039$) during sunitinib withdrawal. *Objective responders* (n = 5) appeared to have a trend towards unchanged SUV_{mean} (+0.00%, range: −14 to +8%; $p = 0.648$) and SUV_{max} (+2.6%, range: −33 to +31%; $p = 0.963$) during sunitinib withdrawal. However, the differences between the responder and non-responder groups were not statistically significant by the Wilcoxon rank sum test.

In an exploratory, unplanned analysis, the association between the changes in SUV parameters and the clinical benefit status was evaluated. The clinical benefit rate for both groups combined was 32%: 43% for the 4/2 schedule and 18% for the 2/1 schedule. Figures 4a and 4b shows the median change in SUV_{max} and SUV_{mean} over different scan periods for

the *clinical benefit* (CB) and *no clinical benefit* (NCB) groups. Subjects with NCB showed a statistically significant increase in SUV_{mean} (+29%; p = 0.012) and SUV_{max} (+45%; p = 0.039) during sunitinib withdrawal. Subjects with CB showed only a trend towards no change in SUV_{mean} (+0.7%; p = 0.238), and a trend towards increase in SUV_{max} (+21%; p = 0.278). Figure 4 visually suggests that relative lack of withdrawal flare (peak exposure to washout) might predict CB, while a larger withdrawal flare appeared to correlate with a decreased chance of clinical benefit (e.g. NCB). However, the differences in median SUV change during sunitinib withdrawal between the CB and NCB groups were not statistically significant by the Wilcoxon rank sum test.

Discussion

Anti-angiogenic strategies are incorporated as treatment for many oncologic diseases, and studies to further optimize their use are ongoing. Despite hundreds of clinical trials, we still do not have a complete understanding of why some patients fail to respond to VEGF Signaling Pathway (VSP) inhibitors and other patients, despite initially responding to treatment, later progress on VSP therapy. We have learned through trial and error that bevacizumab is most effective when combined with other agents (e.g. cytotoxic chemotherapy). Most surprising is that despite higher single-agent activity with VEGFR TKI agents (compared to bevacizumab alone), trials reported to date combining VEGFR TKI agents with cytotoxic chemotherapy have not shown the same promise. Phase III trials of carboplatin/paclitaxel with or without sorafenib in both advanced melanoma(34) and NSCLC,(35) gemcitabine with or without axitinib in pancreatic cancer,(36) and sunitinib with or without FOLFIRI in mCRC(37) have all failed to show an improvement in the primary endpoint with the addition of a VEGFR TKI. Furthermore, patients with squamous histology in the NSCLC trial appeared to have *increased* mortality on the sorafenib-chemotherapy arm compared with the placebo-chemotherapy arm.

It was postulated by Teicher in 1996 that combined administration of anti-angiogenic and cytotoxic therapies would yield maximal benefit, because such combinations would destroy two separate compartments of tumors – cancer cells and endothelial cells.(38) This hypothesis was supported by the clinical data showing that bevacizumab treatment resulted in a significant increase of 5 months in overall survival in patients with metastatic colorectal cancer, when given in combination with standard chemotherapy,(4) whereas as a single agent, it produced only modest objective responses.(2, 18) Jain in 2001 also proposed that judicious application of anti-angiogenic agents can normalize the abnormal tumor vasculature, resulting in more efficient delivery of drugs and oxygen to the targeted cancer cells, and therefore enhancing the effectiveness of chemotherapy and radiation.(39) However, excessive vascular regression may be counterproductive as it compromises drug and oxygen delivery.

A *normalization window*, or a period during which the blood vessels become normalized, is the theoretically optimal time when the addition of chemotherapy or radiotherapy to anti-angiogenic therapy should yield the best therapeutic outcome.(40) A novel study using dynamic-contrast enhance magnetic resonance imaging (DCE-MRI) showed improved tumor perfusion, indicating normalization of blood vessels, in a murine RCC model after 3 days of sunitinib administration, but not after 1 day of sunitinib administration; mice were subsequently treated with weekly gemcitabine.(41) This study suggests that chemotherapy combination with anti-angiogenic therapy may be optimized through the use of functional imaging. Understanding how VEGFR TKI therapy may antagonize cytotoxic chemotherapy was another important goal during the analysis of our study, as ongoing trials combining newer VEGFR TKIs with chemotherapy continue.

Here we show that nearly all patients with advanced solid malignancies have some initial reduction in tumor proliferation as measured by FLT PET/CT after 4 weeks of sunitinib treatment. This reduction was more apparent on the 4/2 schedule versus 2/1 schedule, and more significant for the FLT PET SUV_{max} then SUV_{mean}, which is likely due to a greater duration of sunitinib exposure. Nevertheless, in both schedules, during the brief treatment break patients experienced a relative increase in FLT uptake consistent with an increase in tumor proliferation during the treatment withdrawal period. This finding supports our hypothesis and was seen in both the patients with renal cell cancer as well as other solid malignancies. Because of the longer exposure to sunitinib and longer treatment break, we would have predicted that the 4/2 schedule would have a larger "withdrawal flare," but this was not the case. This may simply be due to the low number of patients assessed; however, a complex relationship between the clinical flare, sunitinib PK, and circulating VEGF could also be playing a role. We are addressing this question in currently on-going trials using a VEGFR TKI with a shorter half-life (e.g. NCT00859118).

During sunitinib exposure, it was observed that most (but not all) patients had some decline in SUV (Figure 3). Looking at the individual patients (dotted lines), one can begin to appreciate the differences in response. Possible categories include those patients that experience no change or a small increase in SUV (proliferation) while on sunitinib but still experience a sunitinib withdrawal flare where SUV greatly increases; individuals where an initial decline in SUV is seen during sunitinib exposure but during withdrawal have an increase in proliferation; and individuals where no apparent change in SUV is seen during/ after sunitinib treatment. In an attempt to link these observations with clinical outcomes (challenging given heterogeneous disease population and low numbers of patients), we conducted an exploratory analysis to evaluate the association between changes in SUV and the CB. As shown in Figures 4a and b, changes in SUV parameters suggest that those with lack of clinical benefit have a larger proliferative flare. Looking at the individual patient data (dotted lines), one can appreciate that initial steep declines in SUV during sunitinib treatment do not always correlate with clinical benefit. Our explanation for these findings is that sunitinib has both anti-angiogenic and anti-tumor activity in most solid tumors as evidenced by a decrease in FLT PET uptake in most patients. Treatment leads to increased physiological hypoxia, which results in a compensatory increase in proangiogenic factors, resulting in angiogenic escape. Thus, the greater ability of the host (patient) to compensate for treatment-induced hypoxia, the more likely that the patient will experience early sunitinib treatment failure. On the other hand, if the host cannot robustly compensate for treatment-induced hypoxia, then angiogenic escape is less likely to occur. The implications of this are enormous: this may provide a rationale to test anti-angiogenic combinations in order to ameliorate this compensatory response and personalize treatment by appropriate dosing schedule.

Our data suggests that the sunitinib withdrawal flare correlates with shorter duration of clinical benefit, and that the largest contributor on univariate and multivariate analysis to drive the flare is plasma VEGF ligand level. It has been observed that baseline VEGF levels gradually increase with chronic sunitinib exposure.(42) While this may be an explanation for eventual treatment failure, the obvious implication is that we do have agents that can target VEGF ligand (e.g. bevacizumab). While studies testing the concurrent combination of sunitinib with bevacizumab have raised concerns regarding overlapping toxicities,(43, 44) suggestions of increased antitumor activity were seen. This raises the question of whether a "sequential" approach can be used to minimize overlapping toxicity and prolong benefit. Our current data has resulted in an ongoing study titled a "Phase I Study of Sequential Sunitinib and Bevacizumab in Patients with Metastatic Renal Cell Carcinoma and Other Advance Solid Malignancies" (NCT01243359) testing *sequential* sunitinib with bevacizumab. Sunitinib is administered on the standard 4/2 schedule, with low-dose

bevacizumab given on day 29 (at start of the 2 week treatment withdrawal) to suppress flare and cycles repeated every 6 weeks. FLT PET/CT imaging is being planned to see if the addition of low-dose bevacizumab will suppress the proliferative flare during sunitinib withdrawal.

One question that might be raised is whether the change in FLT PET uptake we observe is a reflection of tumor proliferation or simply vascular effect (e.g., decreased perfusion in tumor results in decreased tracer delivery resulting in lower FLT uptake). In order to address this question, we performed dynamic FLT PET/CT imaging. Using compartmental modeling (intravascular, extravascular, intracellular), one can calculate K_i, which reflects the proliferative rate when corrected for K_1, which represents the vascular permeability/perfusion (45). In summary, the FLT PET SUV and FLT PET K_i trends were the same, indicating that FLT PET SUV analysis does adequately represent proliferative activity, which is consistent with both clinical and anatomic imaging observations.

In summary, we have shown that during sunitinib treatment on both the 4/2 and 2/1 schedules there are statistically significant increases in median sunitinib concentrations and median serum VEGF levels, and a median decrease in cellular proliferation as measured by SUV_{mean} and SUV_{max}. Change in VEGF during sunitinib treatment predicted change in SUV_{mean} during sunitinib withdrawal, which fits with the biologically plausible hypothesis that the rise in VEGF ligand during treatment may drive tumor flare during the withdrawal period. Finally, there was a suggestion of a more brisk proliferative flare in non-responders compared to responders. This suggests that patients with a robust compensatory response to treatment-induced hypoxia (e.g. large flare) might develop early treatment failure as a result.

Acknowledgments

Sponsored by: CTEP/NCI

Support: Clinical conduct of this study was supported by NCI UO1 CA062491 (Early Clinical Trials of Anti-Cancer Agents with Phase I Emphasis) and NIH/NCI P30 CA014520 (UW Comprehensive Cancer Center Support). FLT PET/CT costs were funded through a Pfizer Oncology Investigator-Initiated Research Grant (GA6180ST). D rs. Harrison, Chao and Vanderhoek were supported by NIH/NCI grants K12 CA087718, T32 CA009614-20, and T32 CA009206 respectively.

The authors would like to thank the nurses and research specialists of the UWCCC Phase I Program for their efforts in conducting and managing this trial, as well as to our patients for their participation in this study and contributions to this research.

References

1. Folkman J. Tumor angiogenesis: therapeutic implications. N Engl J Med. 1971; 285:1182–6. [PubMed: 4938153]
2. Cobleigh MA, Langmuir VK, Sledge GW, Miller KD, Haney L, Novotny WF, et al. A phase I/II dose-escalation trial of bevacizumab in previously treated metastatic breast cancer. Semin Oncol. 2003; 30:117–24. [PubMed: 14613032]
3. Gordon MS, Margolin K, Talpaz M, Sledge GW Jr, Holmgren E, Benjamin R, et al. Phase I safety and pharmacokinetic study of recombinant human anti-vascular endothelial growth factor in patients with advanced cancer. J Clin Oncol. 2001; 19:843–50. [PubMed: 11157038]
4. Hurwitz H, Fehrenbacher L, Novotny W, Cartwright T, Hainsworth J, Heim W, et al. Bevacizumab plus irinotecan, fluorouracil, and leucovorin for metastatic colorectal cancer. N Engl J Med. 2004; 350:2335–42. [PubMed: 15175435]
5. Giantonio BJ, Catalano PJ, Meropol NJ, O'Dwyer PJ, Mitchell EP, Alberts SR, et al. Bevacizumab in combination with oxaliplatin, fluorouracil, and leucovorin (FOLFOX4) for previously treated metastatic colorectal cancer: results from the Eastern Cooperative Oncology Group Study E3200. J Clin Oncol. 2007; 25:1539–44. [PubMed: 17442997]

6. Sandler A, Gray R, Perry MC, Brahmer J, Schiller JH, Dowlati A, et al. Paclitaxel-carboplatin alone or with bevacizumab for non-small-cell lung cancer. N Engl J Med. 2006; 355:2542–50. [PubMed: 17167137]
7. Escudier B, Eisen T, Stadler WM, Szczylik C, Oudard S, Siebels M, et al. Sorafenib in advanced clear-cell renal-cell carcinoma. N Engl J Med. 2007; 356:125–34. [PubMed: 17215530]
8. Motzer RJ, Hutson TE, Tomczak P, Michaelson MD, Bukowski RM, Rixe O, et al. Sunitinib versus interferon alfa in metastatic renal-cell carcinoma. N Engl J Med. 2007; 356:115–24. [PubMed: 17215529]
9. Sternberg CN, Davis ID, Mardiak J, Szczylik C, Lee E, Wagstaff J, et al. Pazopanib in locally advanced or metastatic renal cell carcinoma: results of a randomized phase III trial. J Clin Oncol. 2010; 28:1061–8. [PubMed: 20100962]
10. Motzer RJ, Hutson TE, Tomczak P, Michaelson MD, Bukowski RM, Oudard S, et al. Overall survival and updated results for sunitinib compared with interferon alfa in patients with metastatic renal cell carcinoma. J Clin Oncol. 2009; 27:3584–90. [PubMed: 19487381]
11. Escudier B, Eisen T, Stadler WM, Szczylik C, Oudard S, Staehler M, et al. Sorafenib for treatment of renal cell carcinoma: Final efficacy and safety results of the phase III treatment approaches in renal cancer global evaluation trial. J Clin Oncol. 2009; 27:3312–8. [PubMed: 19451442]
12. Demetri GD, van Oosterom AT, Garrett CR, Blackstein ME, Shah MH, Verweij J, et al. Efficacy and safety of sunitinib in patients with advanced gastrointestinal stromal tumour after failure of imatinib: a randomised controlled trial. Lancet. 2006; 368:1329–38. [PubMed: 17046465]
13. Huang D, Ding Y, Li Y, Luo WM, Zhang ZF, Snider J, et al. Sunitinib acts primarily on tumor endothelium rather than tumor cells to inhibit the growth of renal cell carcinoma. Cancer Res. 70:1053–62. [PubMed: 20103629]
14. Britten CD, Kabbinavar F, Hecht JR, Bello CL, Li J, Baum C, et al. A phase I and pharmacokinetic study of sunitinib administered daily for 2 weeks, followed by a 1-week off period. Cancer Chemother Pharmacol. 2008; 61:515–24. [PubMed: 17505827]
15. Heng DY, Rini BI, Garcia J, Wood L, Bukowski RM. Prolonged complete responses and near-complete responses to sunitinib in metastatic renal cell carcinoma. Clin Genitourin Cancer. 2007; 5:446–51. [PubMed: 18272027]
16. Calvo OF, Vazquez DD, Lopez MR, Aparicio LM. Renal cell carcinoma: complete response. Anticancer Drugs. 21(Suppl 1):S17–8. [PubMed: 20110782]
17. Garcia-Campelo R, Quindos M, Vazquez DD, Lopez MR, Carral A, Calvo OF, et al. Renal cell carcinoma: complete pathological response in a patient with gastric metastasis of renal cell carcinoma. Anticancer Drugs. 21(Suppl 1):S13–5. [PubMed: 20110781]
18. Yang JC, Haworth L, Sherry RM, Hwu P, Schwartzentruber DJ, Topalian SL, et al. A randomized trial of bevacizumab, an anti-vascular endothelial growth factor antibody, for metastatic renal cancer. N Engl J Med. 2003; 349:427–34. [PubMed: 12890841]
19. Bukowski RM, Kabbinavar FF, Figlin RA, Flaherty K, Srinivas S, Vaishampayan U, et al. Randomized phase II study of erlotinib combined with bevacizumab compared with bevacizumab alone in metastatic renal cell cancer. J Clin Oncol. 2007; 25:4536–41. [PubMed: 17876014]
20. Liu G, Jeraj R, Perlman S, Vanderhoek M, Kolesar J, Eickhoff J, et al. Pharmacodynamic study of FLT-PET imaging in patients treated with sunitinib. J Clin Oncol. 2008; 26:abstr 3515.
21. Rugo HS, Herbst RS, Liu G, Park JW, Kies MS, Steinfeldt HM, et al. Phase I trial of the oral antiangiogenesis agent AG-013736 in patients with advanced solid tumors: pharmacokinetic and clinical results. J Clin Oncol. 2005; 23:5474–83. [PubMed: 16027439]
22. Toyohara J, Waki A, Takamatsu S, Yonekura Y, Magata Y, Fujibayashi Y. Basis of FLT as a cell proliferation marker: comparative uptake studies with [3H]thymidine and [3H]arabinothymidine, and cell-analysis in 22 asynchronously growing tumor cell lines. Nucl Med Biol. 2002; 29:281–7. [PubMed: 11929696]
23. Rasey JS, Grierson JR, Wiens LW, Kolb PD, Schwartz JL. Validation of FLT uptake as a measure of thymidine kinase-1 activity in A549 carcinoma cells. J Nucl Med. 2002; 43:1210–7. [PubMed: 12215561]
24. Munch-Petersen B, Cloos L, Jensen HK, Tyrsted G. Human thymidine kinase 1. Regulation in normal and malignant cells. Adv Enzyme Regul. 1995; 35:69–89. [PubMed: 7572355]

25. Barthel H, Cleij MC, Collingridge DR, Hutchinson OC, Osman S, He Q, et al. 3′-deoxy-3′-[18F]fluorothymidine as a new marker for monitoring tumor response to antiproliferative therapy in vivo with positron emission tomography. Cancer research. 2003; 63:3791–8. [PubMed: 12839975]
26. Schwartz JL, Tamura Y, Jordan R, Grierson JR, Krohn KA. Monitoring tumor cell proliferation by targeting DNA synthetic processes with thymidine and thymidine analogs. J Nucl Med. 2003; 44:2027–32. [PubMed: 14660729]
27. Vesselle H, Grierson J, Muzi M, Pugsley JM, Schmidt RA, Rabinowitz P, et al. In vivo validation of 3′deoxy-3′-[(18)F]fluorothymidine ([(18)F]FLT) as a proliferation imaging tracer in humans: correlation of [(18)F]FLT uptake by positron emission tomography with Ki-67 immunohistochemistry and flow cytometry in human lung tumors. Clin Cancer Res. 2002; 8:3315–23. [PubMed: 12429617]
28. Buck AK, Halter G, Schirrmeister H, Kotzerke J, Wurziger I, Glatting G, et al. Imaging proliferation in lung tumors with PET: 18F-FLT versus 18F-FDG. J Nucl Med. 2003; 44:1426–31. [PubMed: 12960187]
29. Mankoff DA, Shields AF, Krohn KA. PET imaging of cellular proliferation. Radiol Clin North Am. 2005; 43:153–67. [PubMed: 15693654]
30. Muzi M, Vesselle H, Grierson JR, Mankoff DA, Schmidt RA, Peterson L, et al. Kinetic analysis of 3′-deoxy-3′-fluorothymidine PET studies: validation studies in patients with lung cancer. J Nucl Med. 2005; 46:274–82. [PubMed: 15695787]
31. Therasse P, Arbuck SG, Eisenhauer EA, Wanders J, Kaplan RS, Rubinstein L, et al. New guidelines to evaluate the response to treatment in solid tumors. European Organization for Research and Treatment of Cancer, National Cancer Institute of the United States, National Cancer Institute of Canada. J Natl Cancer Inst. 2000; 92:205–16. [PubMed: 10655437]
32. de Bruijn P, Sleijfer S, Lam MH, Mathijssen RH, Wiemer EA, Loos WJ. Bioanalytical method for the quantification of sunitinib and its n-desethyl metabolite SU12662 in human plasma by ultra performance liquid chromatography/tandem triple-quadrupole mass spectrometry. J Pharm Biomed Anal. 2010; 51:934–41. [PubMed: 19931354]
33. Thie JA, Hubner KF, Smith GT. The diagnostic utility of the lognormal behavior of PET standardized uptake values in tumors. J Nucl Med. 2000; 41:1664–72. [PubMed: 11037996]
34. Hauschild A, Agarwala SS, Trefzer U, Hogg D, Robert C, Hersey P, et al. Results of a phase III, randomized, placebo-controlled study of sorafenib in combination with carboplatin and paclitaxel as second-line treatment in patients with unresectable stage III or stage IV melanoma. J Clin Oncol. 2009; 27:2823–30. [PubMed: 19349552]
35. Scagliotti G, Novello S, von Pawel J, Reck M, Pereira JR, Thomas M, et al. Phase III study of carboplatin and paclitaxel alone or with sorafenib in advanced non-small-cell lung cancer. J Clin Oncol. 2010; 28:1835–42. [PubMed: 20212250]
36. Kindler HL, Ioka T, Richel DJ, Bennouna J, Letourneau R, Okusaka T, et al. Axitinib plus gemcitabine versus placebo plus gemcitabine in patients with advanced pancreatic adenocarcinoma: a double-blind randomised phase 3 study. Lancet Oncol. 2011; 12:256–62. [PubMed: 21306953]
37. Carrato, A.; Swieboda-Sadlej, A.; Staszewska-Skurczynska, M., et al. Final results from a multicenter, randomized, double-blind, phase 3 study of sunitinib in metastatic colorectal cancer patients receiving irinotecan, 5-fluorouracil and leucovorin (FOLFIRI) as first line treatment. 12th World Congress on Gastrointestinal Cancer, Vol; Barcelona, Spain: European Society of Medical Oncology; 2010. p. Abstr O-0026
38. Teicher BA. A systems approach to cancer therapy (Antioncogenics + standard cytotoxics-->mechanism(s) of interaction). Cancer Metastasis Rev. 1996; 15:247–72. [PubMed: 8842498]
39. Jain RK. Normalizing tumor vasculature with anti-angiogenic therapy: a new paradigm for combination therapy. Nat Med. 2001; 7:987–9. [PubMed: 11533692]
40. Jain RK. Normalization of tumor vasculature: an emerging concept in antiangiogenic therapy. Science. 2005; 307:58–62. [PubMed: 15637262]
41. Hillman GG, Singh-Gupta V, Al-Bashir AK, Zhang H, Yunker CK, Patel AD, et al. Dynamic contrast-enhanced magnetic resonance imaging of sunitinib-induced vascular changes to schedule

chemotherapy in renal cell carcinoma xenograft tumors. Transl Oncol. 2010; 3:293–306. [PubMed: 20885892]

42. Deprimo SE, Bello CL, Smeraglia J, Baum CM, Spinella D, Rini BI, et al. Circulating protein biomarkers of pharmacodynamic activity of sunitinib in patients with metastatic renal cell carcinoma: modulation of VEGF and VEGF-related proteins. J Transl Med. 2007; 5:32. [PubMed: 17605814]
43. Feldman DR, Baum MS, Ginsberg MS, Hassoun H, Flombaum CD, Velasco S, et al. Phase I trial of bevacizumab plus escalated doses of sunitinib in patients with metastatic renal cell carcinoma. J Clin Oncol. 2009; 27:1432–9. [PubMed: 19224847]
44. Rini BI, Garcia JA, Cooney MM, Elson P, Tyler A, Beatty K, et al. A phase I study of sunitinib plus bevacizumab in advanced solid tumors. Clin Cancer Res. 2009; 15:6277–83. [PubMed: 19773375]
45. Jeraj R, Liu G, Simoncic U, Vanderhoek M, Perlman SB, Alberti D, et al. Concurrent Assessment of Vasculature and Proliferative Pharmacodynamics in Patients Treated with VEGFR TKI. J Clin Oncol. 2010; 28:abstr 3050.

Translational Relevance

Inhibiting the VEGF signaling pathway is important when treating patients with advanced cancer. Despite the benefits shown when combining bevacizumab with cytotoxic chemotherapy in certain solid malignancies, investigations combining VEGFR TKIs with cytotoxic chemotherapy have not shown similar promise despite higher single-agent activity of VEGFR TKIs compared to bevacizumab. This has raised questions whether concurrent VEGFR TKIs may be diminishing the effect of cytotoxic chemotherapy, and whether alternative dosing strategies may be better. Given the number of newer VEGFR TKIs in development, understanding of the pharmacodynamics effects of VEGFR TKIs in patients is needed. Here we present a pharmacodynamics study using FLT PET/CT in patients treated with sunitinib. This study provides new insight into the VEGFR TKI withdrawal flare and how this knowledge may be incorporated into more optimal sequencing strategies with these agents. Additionally, this study highlights the power of using functional imaging to assist in early drug development.

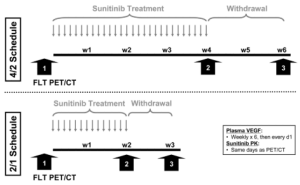

Figure 1.

Schema of pharmacodynamic and pharmacokinetics time points. Patients were administered sunitinib 50 mg daily on the intermittently dosed *4/2 schedule* (top) or *2/1 schedule* (bottom). FLT PET/CT images were performed at baseline, peak sunitinib exposure, and during sunitinib withdrawal as indicated by the wide arrows. *FLT*, ^{18}F-Fluorothymidine. *PET*, positron emission tomography. *CT*, computed tomography. *VEGF*, vascular endothelial growth factor. *PK*, pharmacokinetics. *w*, week.

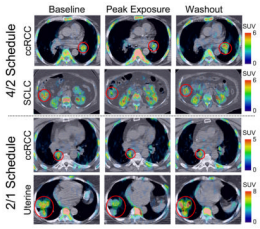

Figure 2.
Examples of the tumor flare phenomenon on FLT PET/CT in various tumor types. *ccRCC*, clear cell renal cell carcinoma. *SCLC*, small cell lung cancer. *SUV*, standardized uptake value.

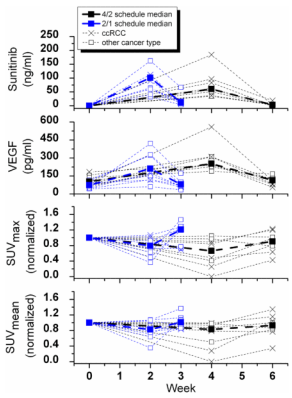

Figure 3.
Pharmacokinetic and pharmacodynamic parameters at time points throughout the sunitinib cycle. *ccRCC*, clear cell renal cell carcinoma. Thin dotted lines show individual patients results.

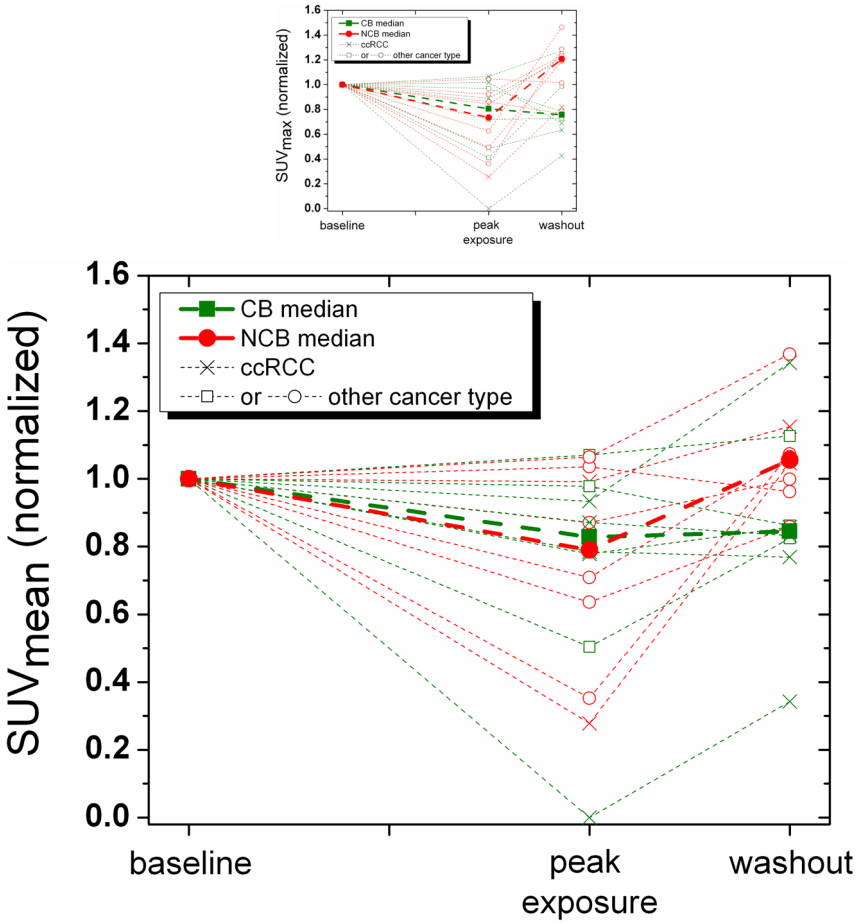

Figure 4.

Figures 4a and b: Change in SUV_{mean} and SUV_{max} (normalized to baseline) by clinical benefit group. Note that the 4/2 and 2/1 schedules are combined so that the abscissa is scaled to sunitinib exposure (and scan time points) instead of time. *CB*, clinical benefit. *NCB*, no clinical benefit. *ccRCC*, clear cell renal cell carcinoma.

Table 1

Changes in pharmacokinetic and pharmacokinetic parameters during the sunitinib treatment and withdrawal periods. The Wilcoxon signed rank test was used for comparing the change between time points during each period. Percent change was used for SUV_{mean} and SUV_{max}, whereas absolute changes were used for all other values. Css, concentration at steady state; met, metabolite.

	4/2 Schedule (n=8)				**2/1 Schedule (n=8)**			
	Treatment		**Withdrawal**		**Treatment**		**Withdrawal**	
	Median Change (Range)	**p-value**	**Median Change (Range)**	**p-value**	**Median Change (Range)**	**p-value**	**Median Change (Range)**	**p-value**
Sunitinib, Css (ng/mL)	**63 (37 – 184)**	0.005	**−59 (−181 — −32)**	0.008	**62 (−32 – 162)**	0.008	**−51 (−104 — −23)**	0.008
Sunitinib met, Css (ng/mL)	**20 (14 – 39)**	<0.001	**−18 (−29 — −5)**	0.008	**21 (5 – 52)**	0.008	**−16 (−26 — −1)**	0.008
VEGF (pg/mL)	**168 (51 – 461)**	0.008	**−184 (−448 — −22)**	0.008	**100 (18 – 361)**	0.008	**−96 (−253 — −26)**	0.008
SUV_{mean} (% change)	**−16 (−100 — 0)**	0.031	**15 (−14 – 277)**	0.047	−18 (−64 — 6)	0.109	**19 (−5 – 200)**	0.047
SUV_{max} (% change)	**−34 (−100 — 4)**	0.016	33 (−18 – 221)	0.078	**−21 (−64 — 6)**	0.039	28 (−33 – 251)	0.109

Table 2

Correlations between changes (Δ) in the various pharmacodynamic and pharmacokinetic parameters during sunitinib treatment and withdrawal periods. Associations between changes in the various pharmacokinetic and pharmacodynamic (PD) parameters were analyzed using Spearman's rank correlation (r_s) analysis.

		4/2 Schedule (n = 8)		2/1 Schedule (n = 8)	
	Sunitinib Period	**Correlation Coefficient**	**p-value**	**Correlation Coefficient**	**p-value**
ΔSunitinib Conc. (metabolite) vs. ΔSUV_{mean}	Treatment	−0.47	0.289	0.20	0.800
	Withdrawal	0.52	0.183	−0.70	0.188
ΔSunitinib Conc. (metabolite) vs. ΔSUV_{max}	Treatment	−0.61	0.148	0.80	0.200
	Withdrawal	0.31	0.456	−0.20	0.747
ΔSunitinib Concentration vs. ΔSUV_{mean}	Treatment	**−0.85**	0.016	− 0.40	0.600
	Withdrawal	0.14	0.736	−0.60	0.285
ΔSunitinib Concentration vs. ΔSUV_{max}	Treatment	−0.64	0.119	**1.00**	0.000
	Withdrawal	0.02	0.955	0.10	0.873
ΔVEGF vs. ΔSUV_{mean}	Treatment	**−0.92**	0.003	0.40	0.600
	Withdrawal	−0.21	0.610	**−0.90**	0.037
ΔVEGF vs. ΔSUV_{max}	Treatment	**−0.79**	0.036	0.40	0.600
	Withdrawal	−0.24	0.570	−0.60	0.285
ΔVEGF vs. ΔSunitinib Concentration	Treatment	**0.82**	0.023	0.40	0.600
	Withdrawal	**0.83**	0.010	0.50	0.391
ΔVEGF vs. ΔSunitinib Concentration (metabolite)	Treatment	0.43	0.337	0.80	0.200
	Withdrawal	0.40	0.320	0.60	0.285